Hindawi Publishing Corporation
International Journal of Antennas and Propagation
Volume 2016, Article ID 8210781, 9 pages
http://dx.doi.org/10.1155/2016/8210781

Research Article

A Single-Point-Fed Wideband Circularly Polarized Rectangular Dielectric Resonator Antenna

Deqiang Yang, Meng Zou, and Jin Pan

Department of Microwave Engineering, School of Electronic Engineering, University of Electronic Science and Technology of China (UESTC), Chengdu 611731, China

Correspondence should be addressed to Meng Zou; zm.1598@163.com

Received 18 October 2015; Revised 10 December 2015; Accepted 24 December 2015

Academic Editor: Ikmo Park

A single-point-fed circularly polarized (CP) rectangular dielectric resonator antenna (DRA) with wide CP bandwidth is presented. By using TE_{111} and TE_{113} modes of the rectangular DRA, a wideband CP performance is achieved. The coupling slot of the antenna contains a resistor loaded monofilar-spiral-slot and four linear slots. Design concept of the proposed antenna is demonstrated by simulations, and parameter studies are carried out. Prototype of the proposed antenna was fabricated and measured. Good agreement between the simulation and measurement is obtained. The measured impedance bandwidth ($|S_{11}| < -10$ dB) and 3 dB axial-ratio (AR) bandwidth are 51.4% (1.91–3.23 GHz) and 33.0% (2.15–3.00 GHz), respectively.

1. Introduction

Dielectric resonator antenna (DRA) [1–4] is a good candidate for wireless service equipment due to its attractive characteristics such as small size, wide bandwidth, and high radiation efficiency.

DRAs with circular polarization (CP) performance are more applicable for the wireless systems than the linearly polarized (LP) ones [5–9], because the CP wireless systems can support flexible orientation between the receiving and transmitting antennas. The published CP DRAs can be divided into two classes: single-point-fed [5–7] and dual-point-fed [8, 9] ones. Single-point-fed CP DRA is easy to implement, but its axial-ratio (AR) bandwidth is narrow. Dual-point-fed CP DRA has a wider AR bandwidth, but it needs a complicated power divider. Recently, several single-point-fed CP DRAs with wide 3 dB AR bandwidths have been reported. For example, a CP hollow rectangular DRA with wide AR bandwidth of 12.4% has been reported in [10]. In [11], simple inclined slot fed CP trapezoidal DRA with an AR bandwidth of as wide as 21.5% has been obtained. Single-point-fed wideband CP DRAs can also be realized by using novel feeding structures [12–14]. And in [15], a 3 dB AR bandwidth of 24.6% has been achieved by merging resonances of the DRA and coupling slot.

In recent years, some CP DRAs with wideband [16, 17] and dual-band [18, 19] performances have been realized by taking advantages of the higher order modes of the DRAs. In this letter, a single-point-fed wideband CP rectangular DRA using higher order mode is investigated. The TE_{111} and TE_{113} modes of rectangular DRA are excited by microstrip line through a slot etched on ground plane to achieve wideband CP operation. Ansoft HFSS [20] was used to simulate the performances of the proposed DRA. Parametric studies have also been carried out to investigate the DRA. To verify the simulation, a prototype antenna was fabricated and measured. Reasonable agreement between the simulated and measured results was attained. The measured results show a wide 3 dB AR bandwidth of 33.0% and a wide impedance bandwidth ($|S_{11}| < -10$ dB) of 51.4%.

2. Antenna Structure

Geometry of the single-point-fed wideband CP rectangular DRA is shown in Figure 1. The rectangular DRA has dimensions of $a = b = 22$ mm and $c = 40$ mm, and it is manufactured from a ceramic material with permittivity of $\varepsilon_r = 10$. The substrate ($\varepsilon_{rs} = 2.2$) has a side length of $l_g = 50$ mm and a thickness of $t = 1$ mm. The coupling slot etched on the ground plane consists of a monofilar-spiral-slot and four linear slots.

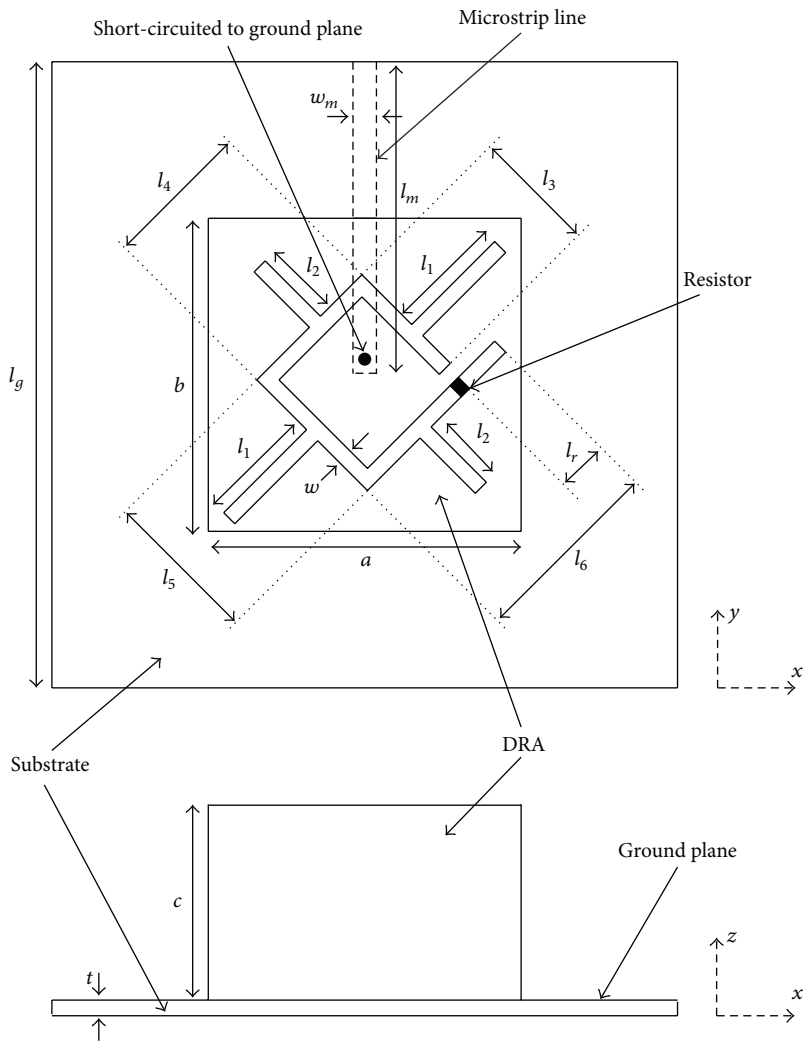

Figure 1: Geometry of the proposed single-point-fed wideband CP rectangular DRA.

3D view Coupling slot Bottom view

Figure 2: Photographs of the fabricated antenna.

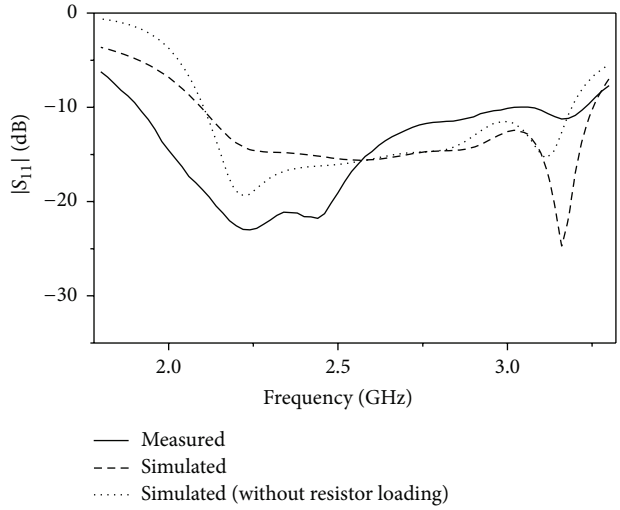

Figure 3: Simulated and measured reflection coefficients of the proposed single-point-fed wideband CP rectangular DRA.

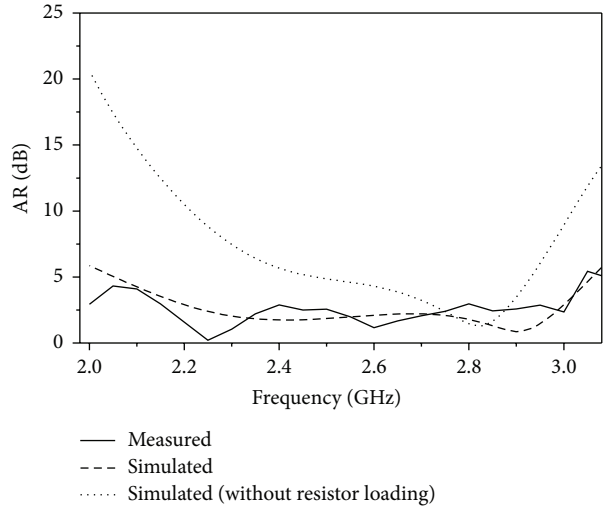

Figure 4: Simulated and measured axial ratios of the proposed single-point-fed wideband CP rectangular DRA.

The width of the slot is $w = 1$ mm. Main side lengths of the monofilar-spiral-slot are $l_3 = 6$ mm, $l_4 = 6$ mm, $l_5 = 7$ mm, and $l_6 = 12$ mm. Lengths of the slot arms located at 45° and 225° with respect to the x-axis are equal to l_1. And the lengths of the other two slot arms located at 135° and 315° with respect to the x-axis are equal to l_2. For the proposed DRA, the lengths of linear slots are $l_1 = 8.0$ mm and $l_2 = 6.8$ mm. A resistor with resistance of $R = 62\ \Omega$ is placed at $l_r = 6$ mm from the end of the slot. The 50 Ω microstrip line ($w_m = 3$ mm, $l_m = 26$ mm) is etched on the other side of substrate, and it is short-circuited to the ground plane at the end.

Resonant frequencies of TE_{111} and TE_{113} modes of the rectangular dielectric resonator (DR) can be calculated by using dielectric waveguide model (DWM) [21] or Ansoft HFSS. The calculated results of the DR in proposed antenna are shown in Table 1. Discrepancies between the two results are caused by error of the DWM.

3. Results

To verify the design, the proposed single-point-fed wideband CP rectangular DRA was fabricated and measured. Photographs of the fabricated antenna are shown in Figure 2. To avoid air gap between the DR and ground plane, the resistor is soldered at the bottom of the substrate by two via holes. Simulated and measured reflection coefficients of the proposed antenna are shown in Figure 3. Measured impedance bandwidth ($|S_{11}| < -10$ dB) is 51.4% (1.91–3.23 GHz), and it agrees well with the simulated one. With reference to Figure 3, there are four resonant frequencies found at 2.24 GHz, 2.44 GHz, 2.84 GHz, and 3.16 GHz across the measured impedance bandwidth. The first couple of resonant frequencies are due to the TE_{111} modes, and the second couple of resonant frequencies are caused by the TE_{113} modes.

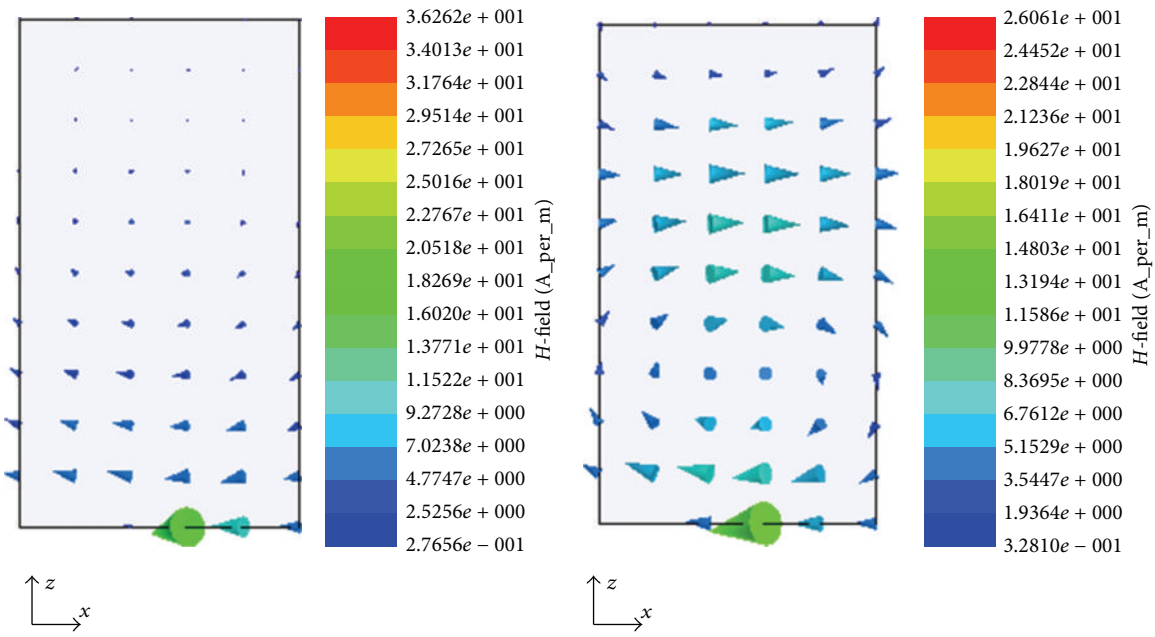

Figure 5: H-fields in the proposed single-point-fed wideband CP rectangular DRA. (a) H-fields at 2.42 GHz. (b) H-fields at 2.90 GHz.

Table 1: Calculated resonant frequencies of TE_{111} and TE_{113} modes of the proposed rectangular DR.

Computing method	TE_{111} mode	TE_{113} mode
DWM	2.42 GHz	3.03 GHz
Ansoft HFSS	2.52 GHz	3.08 GHz

Figure 4 shows the simulated and measured broadside ARs of the proposed antenna. The simulated and measured 3 dB AR bandwidth are 31.2% (2.19–3.00 GHz) and 33.0% (2.15–3.00 GHz), respectively. From Figure 4, two simulated minimum AR values of 1.7 dB and 0.9 dB are obtained at 2.42 GHz and 2.90 GHz, respectively. Simulated H-fields in the proposed DRA at 2.42 GHz and 2.90 GHz are shown in Figures 5(a) and 5(b). H-field distributions demonstrate that the TE_{111} mode is excited at 2.42 GHz and the TE_{113} mode is excited at 2.90 GHz. Figure 6 shows the simulated and measured patterns of the proposed single-point-fed wideband CP rectangular DRA. The radiation patterns of proposed antenna are broadside as expected, because both of the TE_{111} and TE_{113} are broadside modes. And the antenna is RHCP in broadside direction across the CP bandwidth. Figure 7 shows the simulated and measured RHCP gains of the proposed DRA. The measured peak RHCP gain is 6.8 dBi at 2.70 GHz. And the measured result shows an average RHCP gain of 5.4 dBi across the 3 dB AR bandwidth.

4. Parametric Studies

Effects of the resistor on antenna performances are investigated by HFSS simulations. Simulated AR of the proposed DRA without resistor loading is shown in Figure 4. The DRA without resistor has a 3 dB AR bandwidth of 6.1% (2.72–2.89 GHz). And the 3 dB AR bandwidth of the loaded one is about 5.0 times of the unloaded one. Simulated reflection coefficient of the unloaded one is shown in Figure 3. The resistor has a small effect on the reflection coefficient of the proposed antenna. Simulated total efficiencies of the proposed DRA with and without resistor loading are shown in Figure 8. The efficiency of the loaded one is smaller than the unloaded one because of the loss introduced by the resistor. The minimum efficiency and average efficiency of the loaded one across the CP bandwidth are 0.62 and 0.89, respectively. Figure 9 shows the simulated RHCP and LHCP gains of the proposed DRA with and without resistor loading. From Figure 9, the LHCP component drops a lot when the antenna is loaded, and the resistor has a small effect on the RHCP component of the proposed antenna.

To explain the effect of resistor on antenna performance, the electric field $\vec{E_s}$ in the slot is studied. Figure 10 shows the simulated $\vec{E_s}$ at $f = 2.4$ GHz and $f = 2.9$ GHz in different time steps for the antenna without resistor loading. $\vec{E_s}$ is strong at the position of the resistor for $f = 2.4$ GHz, while it is weak at the position of the resistor for $f = 2.9$ GHz. This means that some power will be dissipated in the resistor at 2.4 GHz and very little power will be lost in the resistor at 2.9 GHz when the antenna is loaded, and that is why the resistor has effect on only lower band of the antenna. Moreover, it can be seen that the equivalent magnetic current ($\vec{M_s} = \vec{E_s} \times \hat{Z}$) in the monofilar-spiral-slot at 2.4 GHz is in a travelling waveform. The resistor, which acts as a resistive termination for the monofilar-spiral-slot, can improve travelling wave performance of the equivalent magnetic current and thus the CP performance at the lower band.

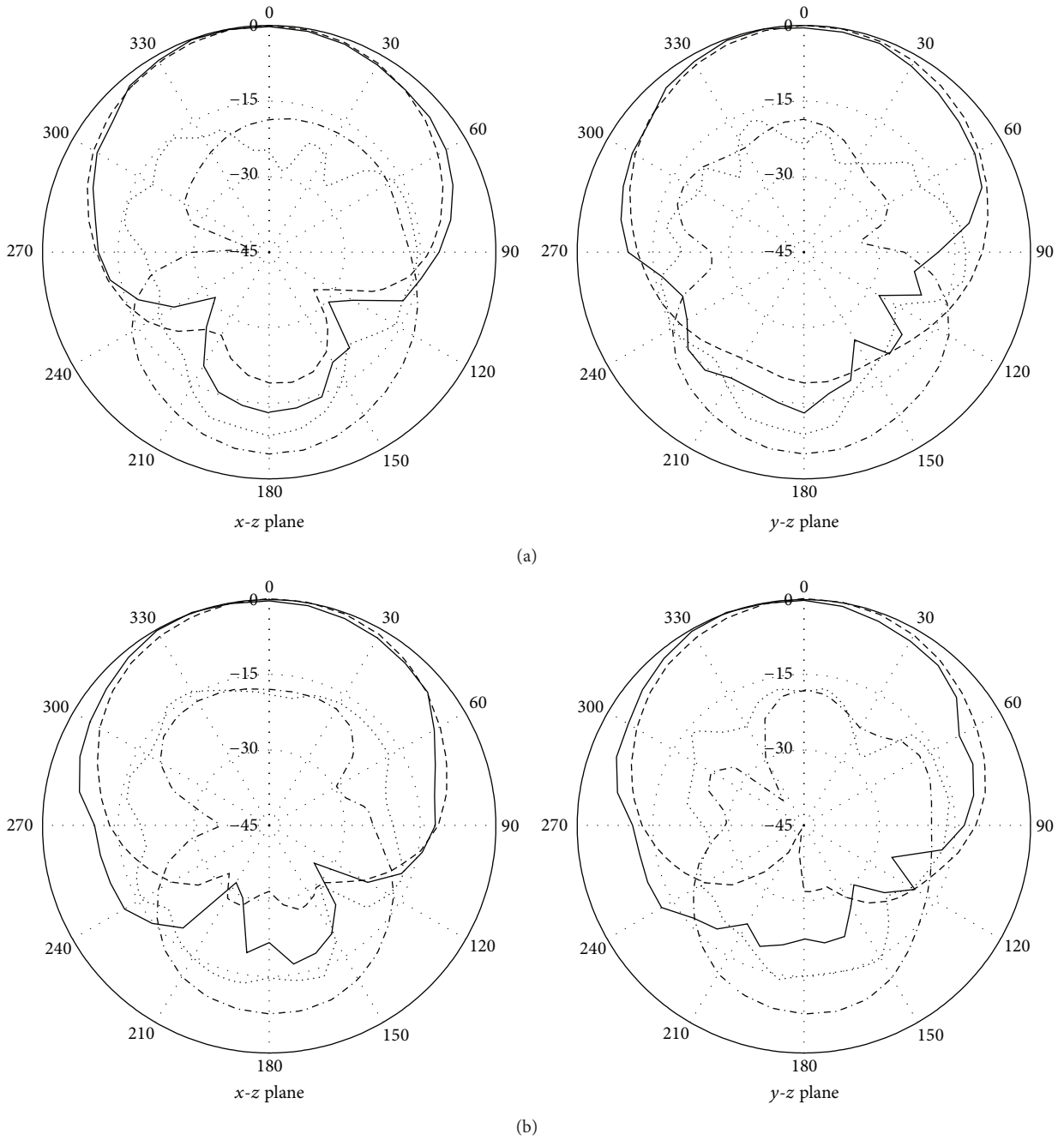

Figure 6: Simulated and measured radiation patterns of the proposed single-point-fed wideband CP rectangular DRA. (a) 2.3 GHz. (b) 2.7 GHz.

The AR and total efficiency for different values of R are shown in Figure 11. With reference to the figure, the widest CP bandwidth is obtained at $R = 60\,\Omega$. And the total efficiency remains almost unchanged when R increases from $20\,\Omega$ to $100\,\Omega$.

Effects of the location of resistor on antenna performances have also been studied. The 3 dB AR bandwidth as function of l_r is shown in Figure 12, and it can be observed that CP bandwidth of the proposed antenna increases with the increase of l_r. Minimum total efficiency and average total efficiency across the 3 dB AR bandwidth versus l_r are also exhibited in Figure 12. From Figure 12, both of the minimum and average total efficiency decrease with the increase of l_r. Proper value of l_r can be decided based on Figure 12 and the special design objectives.

Comparison between the proposed antenna and some of the recently published single-point-fed CP DRAs is listed in Table 2. It is seen that the proposed antenna has a wide bandwidth and reasonable antenna efficiency.

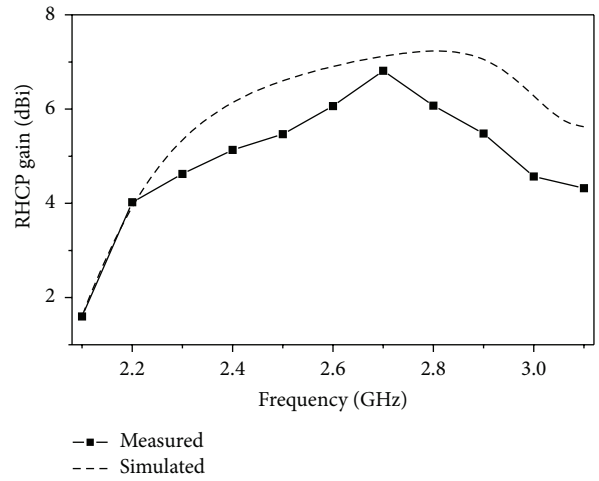

Figure 7: Simulated and measured RHCP gains of the proposed single-point-fed wideband CP rectangular DRA.

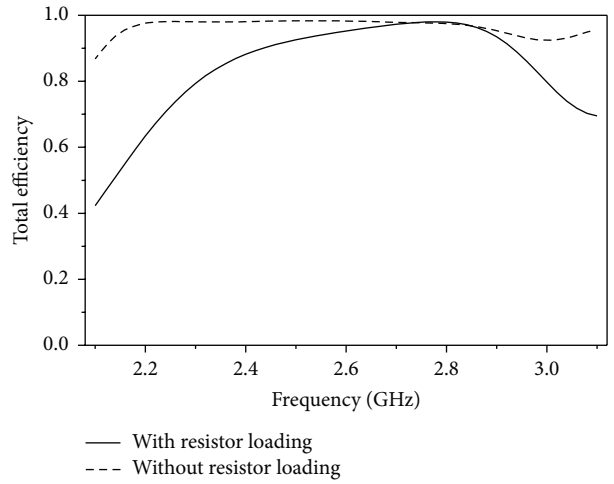

Figure 8: Simulated total efficiencies of the proposed DRA with and without resistor loading.

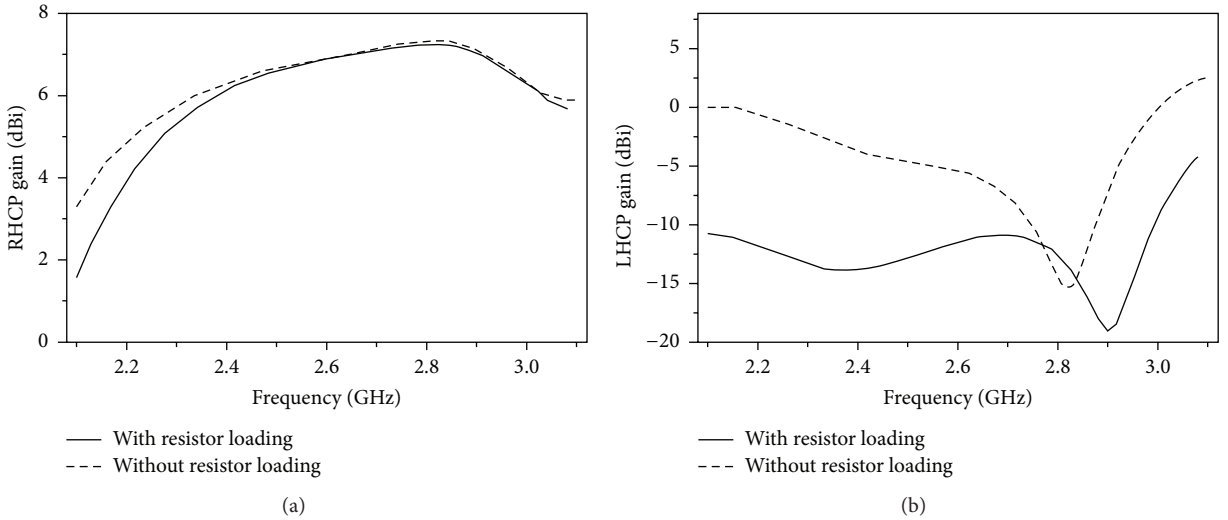

Figure 9: Simulated gains of the proposed DRA with and without resistor loading. (a) RHCP gains. (b) LHCP gains.

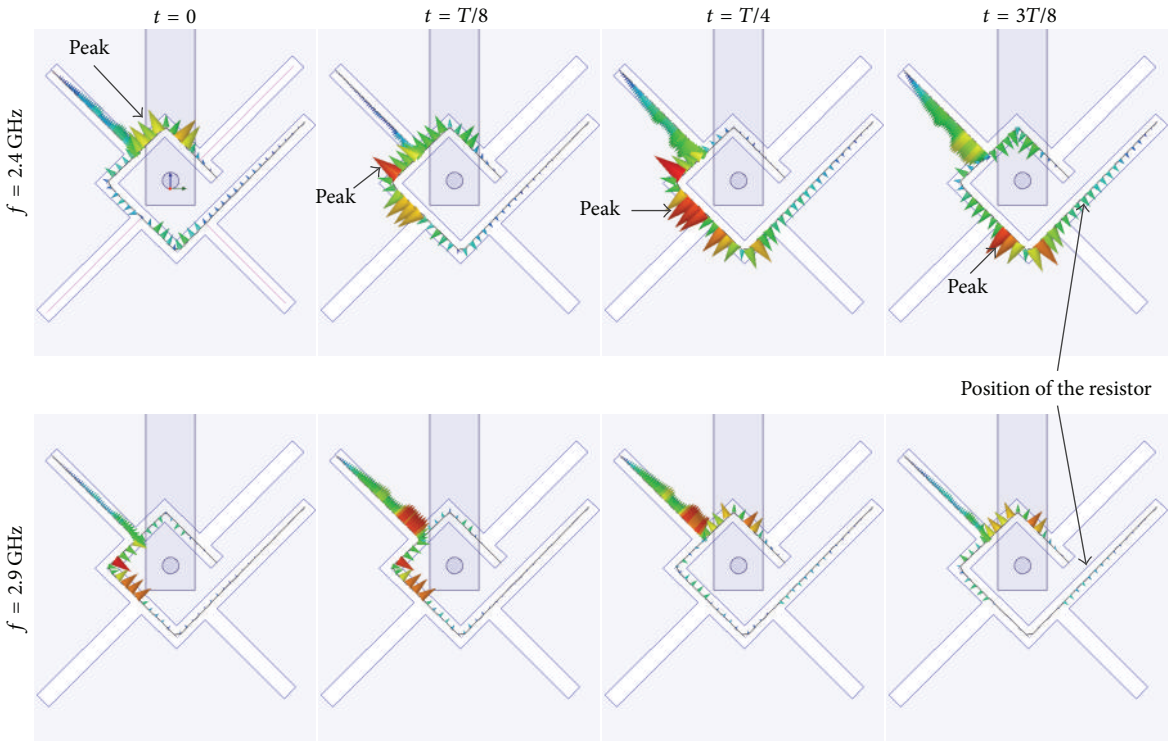

FIGURE 10: Simulated $\overrightarrow{E_s}$ in the slot. ($T = 1/f$).

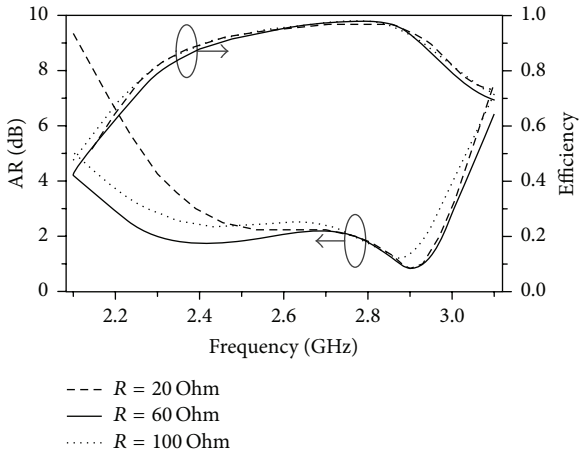

FIGURE 11: AR and total efficiency and for different values of R.

TABLE 2: Comparison between the proposed antenna and other published single-point-fed CP DRAs.

DRA shape	ε_r	3 dB AR bandwidth	Impedance bandwidth	Average total efficiency	Reference
Hollow rectangular	9.4	12.4%	32.5%	—	[10]
Trapezoidal	9.4	21.5%	33.5%	90%	[11]
Rectangular	9.2	14.0%	19.0%	98%	[12]
Rectangular	12	18.7%	53.5%	75%	[13]
Rectangular	12	25.5%	—	82%	[14]
Rectangular	10	33.0%	51.4%	89%	Proposed

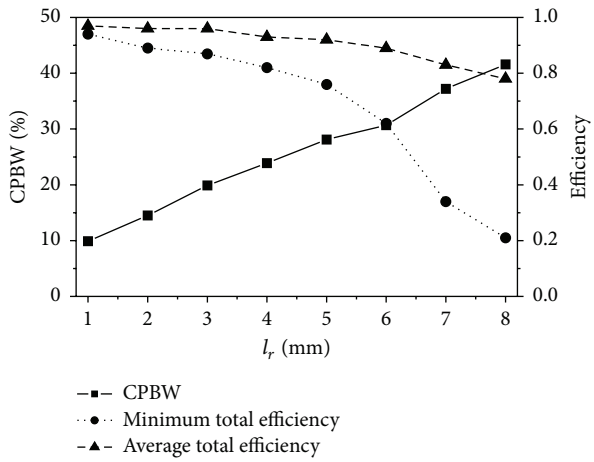

Figure 12: Effects of l_r on AR and total efficiency of the proposed antenna.

5. Conclusion

A single-point-fed wideband CP rectangular DRA has been proposed and discussed in this letter. The design concept is based on utilizing the fundamental TE_{111} and high order TE_{113} modes of rectangular DRA. Proposed design concept has been certified by HFSS simulation. And parametric studies have been carried out to investigate effects of the resistor on antenna performances. A prototype antenna was designed and fabricated. The measured 3 dB AR bandwidth and impedance bandwidth ($|S_{11}| < -10$ dB) are as wide as 33.0% and 51.4%, respectively.

Conflict of Interests

The authors declare that there is no conflict of interests regarding the publication of this paper.

References

[1] S. A. Long, M. W. McAllister, and L. C. Shen, "The resonant cylindrical dielectric cavity antenna," *IEEE Transactions on Antennas and Propagation*, vol. 31, no. 3, pp. 406–412, 1983.

[2] K. M. Luk and K. W. Leung, *Dielectric Resonator Antennas*, Research Studies Press, Baldock, UK, 2003.

[3] K. W. Leung, E. H. Lim, and X. S. Fang, "Dielectric resonator antennas: from the basic to the aesthetic," *Proceedings of the IEEE*, vol. 100, no. 7, pp. 2181–2193, 2012.

[4] R. K. Mongia and A. Ittipiboon, "Theoretical and experimental investigations on rectangular dielectric resonator antennas," *IEEE Transactions on Antennas and Propagation*, vol. 45, no. 9, pp. 1348–1356, 1997.

[5] C.-Y. Huang, J. Y. Wu, and K. L. Wong, "Cross-slot-coupled microstrip antenna and dielectric resonator antenna for circular polarization," *IEEE Transactions on Antennas and Propagation*, vol. 47, no. 4, pp. 605–609, 1999.

[6] K. W. Leung and H. K. Ng, "Theory and experiment of circularly polarized dielectric resonator antenna with a parasitic patch," *IEEE Transactions on Antennas and Propagation*, vol. 51, no. 3, pp. 405–412, 2003.

[7] G. Almpanis, C. Fumeaux, and R. Vahldieck, "Offset cross-slot-coupled dielectric resonator antenna for circular polarization," *IEEE Microwave and Wireless Components Letters*, vol. 16, no. 8, pp. 461–463, 2006.

[8] K. W. Leung, W. C. Wong, K. M. Luk, and E. K. N. Yung, "Circular-polarised dielectric resonator antenna excited by dual conformal strips," *Electronics Letters*, vol. 36, no. 6, pp. 484–486, 2000.

[9] R.-C. Han, S.-S. Zhong, and J. Liu, "Broadband circularly polarised dielectric resonator antenna fed by wideband switched line coupler," *Electronics Letters*, vol. 50, no. 10, pp. 725–726, 2014.

[10] K. Lu, K. W. Leung, and Y. M. Pan, "Theory and experiment of the hollow rectangular dielectric resonator antenna," *IEEE Antennas and Wireless Propagation Letters*, vol. 10, pp. 631–634, 2011.

[11] Y. Pan and K. W. Leung, "Wideband circularly polarized trapezoidal dielectric resonator antenna," *IEEE Antennas and Wireless Propagation Letters*, vol. 9, pp. 588–591, 2010.

[12] M. I. Sulaiman and S. K. Khamas, "A singly fed wideband circularly polarized dielectric resonator antenna using concentric open half-loops," *IEEE Antennas and Wireless Propagation Letters*, vol. 10, pp. 1305–1308, 2011.

[13] M. Zou, J. Pan, Z. Nie, and P. Li, "A wideband circularly polarized rectangular dielectric resonator antenna excited by a lumped resistively loaded monofilar-spiral-slot," *IEEE Antennas and Wireless Propagation Letters*, vol. 12, pp. 1646–1649, 2013.

[14] M. Zou, J. Pan, and Z. Nie, "A wideband circularly polarized rectangular dielectric resonator antenna excited by an archimedean spiral slot," *IEEE Antennas and Wireless Propagation Letters*, vol. 14, pp. 446–449, 2015.

[15] M. Zou and J. Pan, "Wideband hybrid circularly polarised rectangular dielectric resonator antenna excited by modified cross-slot," *Electronics Letters*, vol. 50, no. 16, pp. 1123–1125, 2014.

[16] B. Li, C.-X. Hao, and X.-Q. Sheng, "A dual-mode quadrature-fed wideband circularly polarized dielectric resonator antenna," *IEEE Antennas and Wireless Propagation Letters*, vol. 8, pp. 1036–1038, 2009.

[17] X. S. Fang and K. W. Leung, "Linear-/circular-polarization designs of dual-/wide-band cylindrical dielectric resonator antennas," *IEEE Transactions on Antennas and Propagation*, vol. 60, no. 6, pp. 2662–2671, 2012.

[18] M. Zhang, B. Li, and X. Lv, "Cross-slot-coupled wide dual-band circularly polarized rectangular dielectric resonator antenna," *IEEE Antennas and Wireless Propagation Letters*, vol. 13, pp. 532–535, 2014.

[19] X. Fang, K. W. Leung, and E. H. Lim, "Singly-fed dual-band circularly polarized dielectric resonator antenna," *IEEE Antennas and Wireless Propagation Letters*, vol. 13, pp. 995–998, 2014.

[20] Ansoft high frequency structure simulator (HFSS), ver. 12.0, Ansoft corp, 2009.

[21] R. K. Mongia, "Theoretical and experimental resonant frequencies of rectangular dielectric resonators," *IEE Proceedings Microwaves, Antennas and Propagation*, vol. 139, no. 1, pp. 98–104, 1992.